Interlayer coupling of Fe/Si/Fe trilayers with very thin boundary layers

Y. Endo,[a] O. Kitakami, and Y. Shimada
Research Institute for Scientific Measurements, Tohoku University, 2-1-1 Katahira, Aoba-ku, Sendai 980-8577, Japan

The interlayer magnetic coupling of a Fe/Si/Fe trilayer shows an analogous feature to that of Fe/Si superlattices. With an increase in Si layer thickness, it oscillates as ferromagnetic (first *F*), antiferromagnetic (AF), ferromagnetic (second *F*), and finally reaches a noncoupling (*N*) state. We have investigated interlayer coupling of Fe/Si/Fe trilayers inserting very thin (1 or 2 ML thick) boundary layers X (X=Ag, Ge, Fe–Si, Ta, etc.). They are expected to suppress interatomic diffusion between Fe and Si layers. Interlayer coupling of Fe/X/Si/X/Fe with negligible interdiffusion is simply *F* and changes to *N* as the Si layer thickness increases. Furthermore, Fe/Fe–Si/Fe trilayers which show coupling of first *F*, AF but not second *F*, reproduce second *F* when a Si layer is inserted in the Fe–Si spacer. These results imply that an amorphous Si spacer mediates ferromagnetic coupling between neighboring Fe layers while the first *F* and the strong AF coupling usually observed in Fe/Si superlattices are caused by diffused crystalline Fe–Si. © *1999 American Institute of Physics.* [S0021-8979(99)45508-2]

INTRODUCTION

Since finding of antiferromagnetic (AF) coupling in Fe/Si/Fe trilayers by Toscano *et al.*,[1] magnetic coupling between adjacent Fe layers in Fe/Si superlattices has been investigated by many authors.[2–8] However, in spite of numerous efforts, the origin of the interlayer coupling in this system has not been clarified. We found that the strong AF coupling in this system should be attributed to a nonmagnetic Fe–Si interdiffused layer formed at the interface.[9,10] However, according to the cross-sectional transmission electron microscopy, there coexist both diffused Fe–Si alloy and thin amorphous Si (*a*-Si) within the spacer of the Fe/Si superlattices, and it is of interest to determine if this *a*-Si is another cause of the interlayer coupling in this system.

In this article, we fabricated Fe/Si/Fe trilayers and Fe/X/Si/X/Fe pentalayers. Here, X (X=Ag, Ge, Fe–Si, Ta, etc.) was inserted into the Fe/Si interface to suppress interdiffusion at the Fe/Si interface. Thus, we expected formation of a very thin and homogeneous *a*-Si layer without the coexistence of Fe–Si diffused layer.

EXPERIMENTAL PROCEDURE

A series of Fe/Si/Fe trilayers and Fe/X/Si/X/Fe pentalayers were grown on the surface oxidized Si(100) substrates at ambient temperature in a dc magnetron sputtering system, with a base pressure lower than 6.0×10^{-7} Torr and an argon gas pressure of 3 mTorr. Fe/$Fe_{1-x}Si_x$/Fe ($x=0.54,0.63$) and Fe/X/Fe trilayers were also fabricated for comparison. The electric conductivity of the $Fe_{1-x}Si_x$ was found to be metallic in the investigation reported in the past.[9] These trilayers were grown with Fe layer thickness fixed at $t_{Fe}=100$ Å and the nominal spacer (Si, Fe–Si, and X) layer thickness t_{spacer} ranges from 2 to 70 Å. On the other hand, these pentalayers were grown with the Fe layer thickness fixed at $t_{Fe}=100$ Å, the X layer thickness fixed at $t_{spacer}=2$ or 5 Å, and the nominal Si layer thickness t_{Si} varied from 2 to 70 Å. Here, X is a thin boundary layer inserted into the Fe/Si interface and is expected to suppress interdiffusion. We chose nonmagnetic $Fe_{1-x}Si_x$($x>0.50$), Ag, Ge, and Ta as X. The structure of these samples were characterized by x-ray diffraction (XRD) using Cu$K\alpha$ radiation. The crystalline coherence length ξ was estimated from the full width at half maximum (FWHM) of a Fe(110) diffraction peak by using Scherrer's relation.[9] The magnetic properties and interlayer coupling of these samples were measured by a vibrating sample magnetometer (VSM). The interlayer coupling constant J was also evaluated by analyses of FMR spectra.[9] Here, we define $J>0$ as ferromagnetic (*F*) coupling and $J<0$ as AF coupling.

RESULTS AND DISCUSSION

Figure 1 shows the dependence of the remanence ratio M_r/M_s, saturation field H_s, the coherence length ξ, and the coupling constant J on the Si layer thickness in

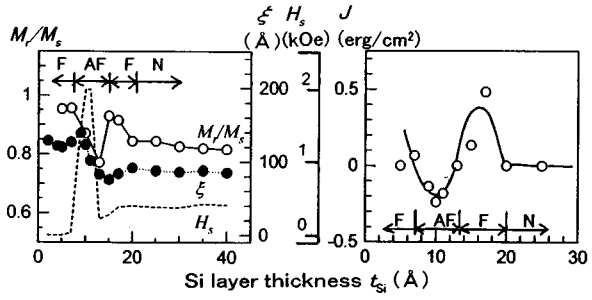

FIG. 1. Dependences of the remanence ratio M_r/M_s, the saturation field H_s, the coherence length ξ, and the interlayer coupling constant J on the Si layer thickness for Fe(100 A)/Si(t_{Si})/Fe(100 Å) trilayers. (F) and (AF) denote ferro and antiferromagnetic coupling, respectively. The solid line in the figure is a guide to the eyes.

[a]Author to whom correspondence should be addressed; electronic mail: endo@rism.tohoku.ac.jp

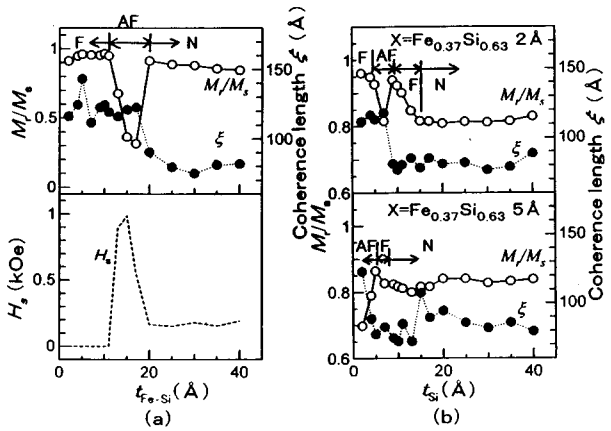

FIG. 2. Dependences of the M_r/M_s and the ξ on the spacer thickness for (a) Fe(100 Å)/$Fe_{0.37}Si_{0.63}$(t_{Fe-Si})/Fe(100 Å) trilayers and (b) Fe(100 Å)/$Fe_{0.37}Si_{0.63}$(t_{Fe-Si})/Si(t_{Si})/$Fe_{0.37}Si_{0.63}$(t_{Fe-Si})/Fe(100 Å) pentalayers (t_{Fe-Si} =2 and 5 Å). (b) (○) and (●), respectively, show the M_r/M_s and the ξ. The broken line in (a) shows the saturation field H_s.

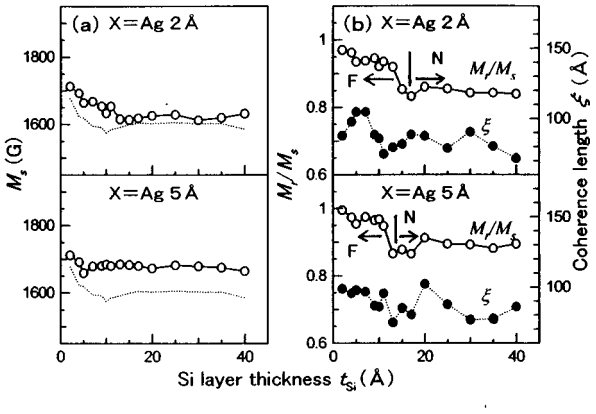

FIG. 3. (a) The saturation magnetization M_s and (b) the remanence ratio M_r/M_s and the coherence length ξ of Fe(100 Å)/Ag(t_{Ag})Si(t_{Si})/Ag(t_{Ag}) Fe(100 Å) pentalayers (t_{Ag}=2 and 5 Å) as functions of t_{Si}. The dotted lines in (a) show the M_s of Fe/Si/Fe trilayers.

Fe(100 Å)/Si(t_{Si} Å)/Fe(100 Å) trilayers. As shown in Fig. 1, the interlayer coupling exhibits a dependence on the spacer thickness similar to that in Fe/Si superlattices;[9] that is, ferromagnetic coupling for $t_{Si}<10$ Å, AF coupling for $10\leqslant t_{Si}\leqslant 13$ Å, and *F* coupling for $13<t_{Si}<20$ Å, and furthermore noncoupling (*N*) for $t_{Si}\geqslant 20$ Å. It should be stressed here that all the coupling behaviors in these samples were confirmed by FMR measurements, and evaluation of the interlayer coupling in terms of M_r/M_s is totally valid. FMR spectra showed a single absorption peak for $t_{Si}<5$ Å, suggesting that two Fe layers are directly connected to each other through pinholes. In contrast, an optical resonance peak was observed for $t_{Si}\geqslant 5$ Å in addition to an acoustic one. Details of the precise analysis of FMR curves of Fe/Si/Fe will be described in the near future. In Fig. 1, the saturation field H_s drastically increases in the AF coupled state. The coherence length decreases down to the Fe layer thickness when $t_{Si}\sim 13$ Å, indicating that the spacer becomes amorphous. At this spacer thickness, the coupling drastically changes from AF to second *F* coupling. Thus the appearance of second *F* coincides with the precipitation of amorphous Si or Fe–Si. This second *F* coupling is not due to a so-called orange-peel effect, because the second *F* coupling strength (0.2–0.5 erg/cm^2) is one order of magnitude higher than that of the magnetostatic coupling.[11]

Figure 2(a) shows that in the Fe/$Fe_{0.37}Si_{0.63}$/Fe trilayer where the Si spacer is purposely replaced by Fe–Si, second *F* coupling is absent in spite of very similar coupling behaviors. Furthermore, as shown by the dotted line in Fig. 2(a), the saturation field H_s drastically increases in the AF coupled state. The coherence length in this trilayer is also analogous to Fe/Si/Fe and limited to less than the Fe layer thickness for $t_{Fe-Si}\geqslant 20$ Å. As this change of the coherence length is the same as the results of Fe/Si/Fe, it indicates that an *a*-Fe–Si spacer is formed at the Fe/$Fe_{0.37}Si_{0.63}$/Fe trilayer for $t_{Fe-Si}\geqslant 20$ Å where the coupling behavior is noncoupling. As a consequence, the *a*-Fe–Si spacer is not a mediator of second *F* coupling in the Fe/Si/Fe trilayer. However, in the Fe/Fe–Si/Si/Fe–Si/Fe pentalayer in Fig. 2(b) where the Fe–Si spacer was inserted at the Fe/Si interface and fixed at 2 or 5 Å, the second *F* coupling reappears. The change of the coherence length in these samples corresponds to that in Fe/Si/Fe. Therefore, the results in Fig. 2 suggest that the second *F* coupling in the Fe/Si/Fe trilayers should be attributed to the formation of an *a*-Si spacer.

Another series of experiments was made to elucidate the role of the *a*-Si layer. We fabricated Fe/X/Si/X/Fe pentalayers where X=Ag, Ge, and Ta. These Xs are expected to suppress atomic interdiffusion between the Fe and Si layers and accelerate formation of an *a*-Si layer. As seen in Fig. 3, insertion of Ag with a thickness of only 2 Å removes AF and second *F* coupling although there still occurs a certain amount M_s reduction. Ag layers with a thickness of 5 Å remove interdiffusion more effectively and a similar trend is observed. The coherence length for these pentalayers is always close to the Fe layer thickness. These results indicate that suppression of interdiffusion accelerates formation of the *a*-Si layer and simply gives rise to *F* coupling, as shown in Fig. 3(b). The similar disappearance of AF and second *F* coupling also occurs when Ta is used as X. In the case of Ge as X, suppression of interdiffusion is less pronounced and the coherence length retains higher values before the Si layer becomes thick enough, as seen in Fig. 4(b). But insertion of a 2 Å thick Ge layer is also effective to remove AF coupling and again *F* coupling is distinct for a Si layer thickness less than 20 Å. These drastic changes of coupling behavior in these pentalayers were also confirmed by FMR measurements, and the details of FMR measurements will be described elsewhere.[12]

Suppression of interdiffusion by Ge stimulated us to investigate Fe/Ge/Fe trilayers since Ge is another intrinsic semiconductor and analogous to the electric properties of Si, as described below. Figure 5 shows results of Fe/Ge/Fe. Fe/Ge/Fe exhibits very little reduction of M_s, irrespective of the increase of the Ge layer thickness. This is a distinguished difference from Fe/Si/Fe in which a large amount of atomic interdiffusion made the role of the *a*-Si spacer ambiguous. As seen in Fig. 5, the AF and second *F* coupling totally

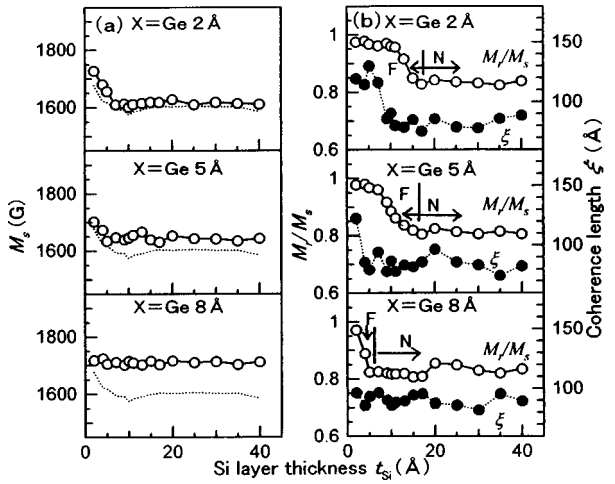

FIG. 4. (a) The M_s and (b) the M_r/M_s and the ξ of Fe(100 Å)/Ge(t_{Ge})/Si(t_{Si})/Ge(t_{Ge})/Fe(100 Å) pentalayers ($t_{Ge}=2$, 5, and 8 Å) as functions of t_{Si}. The dotted lines in (a) show the M_s of Fe/Si/Fe trilayers for comparison.

disappear in Fe/Ge/Fe trilayers. The indirect exchange coupling constants J evaluated from optical modes in the FMR spectra are also given in Fig. 5. They are positive for the Ge layer thickness up to 18 Å reducing to zero for thicker Ge layers. This is consistent with the dependence of M_r/M_s on the Ge layer thickness. Furthermore, variation of ξ in Fig. 5 indicates that the a-Ge layer is formed when Ge layer thickness is more than 10 Å. However, on thinner Ge layers, ξ is somewhat longer. It suggests that very thin Ge layers tend to be crystalline. Therefore, the study of Fe/Fe–Ge/Fe trilayers in which artificial interdiffusion layers are fabricated by replacing Ge with Fe–Ge is expected to give significant information on the role of diffused Fe–Ge layers. This experiment is in preparation.

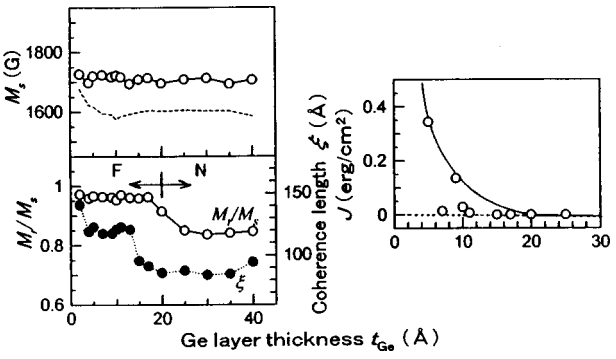

FIG. 5. Dependences of the M_s, the M_r/M_s, the ξ, and the indirect exchange coupling constant J on the Ge layer thickness for Fe(100 Å)/Ge(t_{Gei})/Fe(100 Å) trilayers. The broken line in the left upper panel shows the M_s of Fe/Si/Fe trilayers.

CONCLUSION

We have investigated the interlayer coupling of Fe/Si/Fe trilayers with insertion of various kinds of thin boundary layers (X). In the absence of X, the spacer changes from crystalline to amorphous with an increase of the thickness. The first F and AF coupling appeared when the spacer was in a diffused crystalline state. The coupling drastically changed from AF to second F in accordance with the precipitation of amorphous Si. Moreover, only F coupling was observed when interdiffusion at Fe/Si was entirely suppressed by the insertion of X. These results indicate that the second F observed in Fe/Si trilayers and multilayers is closely related to the presence of a-Si in the spacer.

ACKNOWLEDGMENTS

One of the authors (Y.E.) acknowledges financial support by the Storage Research Consortium in Japan. They are greatly indebted to M. Ichijo for performing FMR measurements. This work was supported by Research for the Future Program of Japan Society for the Promotion of Science under Grant No. 97R14701.

[1] I. S. Toscano, B. Briner, H. Hopster, and M. Landolt, J. Magn. Magn. Mater. **114**, L6 (1992).
[2] E. E. Fullerton, J. E. Mattson, S. R. Lee, C. H. Sowers, Y. Y. Huang, G. Felcher, S. D. Bader, and F. T. Parker, J. Magn. Magn. Mater. **117**, L301 (1992).
[3] A. Chaiken, R. P. Michel, and M. A. Wall, Phys. Rev. B **53**, 5518 (1996).
[4] E. E. Fullerton and S. D. Bader, Phys. Rev. B **53**, 5112 (1996).
[5] J. J. de Vries, J. Kohlhepp, F. J. A. den Broeder, R. Coehoorn, R. Jungblut, A. Reinders, and W. J. M. de Jonge, Phys. Rev. Lett. **78**, 3023 (1997).
[6] K. Inomata, K. Yusu, and Y. Saito, Phys. Rev. Lett. **74**, 1863 (1995).
[7] Y. Endo, O. Kitakami, and Y. Shimada, J. Magn. Soc. Jpn. **21**, 541 (1997).
[8] Y. Endo, O. Kitakami, and Y. Shimada, Appl. Phys. Lett. **72**, 495 (1998).
[9] Y. Endo, O. Kitakami, and Y. Shimada, Phys. Rev. B **59**, 4279 (1999).
[10] Y. Endo, O. Kitakami, and Y. Shimada, IEEE Trans. Magn. **34**, 906 (1998).
[11] The magnetostatic coupling through the orange-peel effect can be easily estimated by Neel's formula. [L. Neel, C. R. Acad. Sci. URSS **255**, 1545 (1962).] Since the amplitude and wavelength of the undulation of our samples are, respectively, $w<10$ Å and $\lambda \geqslant 200$ Å, the coupling strength is on the order of ~ 0.01 erg/cm^2.
[12] Y. Endo, O. Kitakami, and Y. Shimada (unpublished).